iScience

CellPress
OPEN ACCESS

Article

Longitudinal analysis of genomic mutations in SARS-CoV-2 isolates from persistent COVID-19 patient

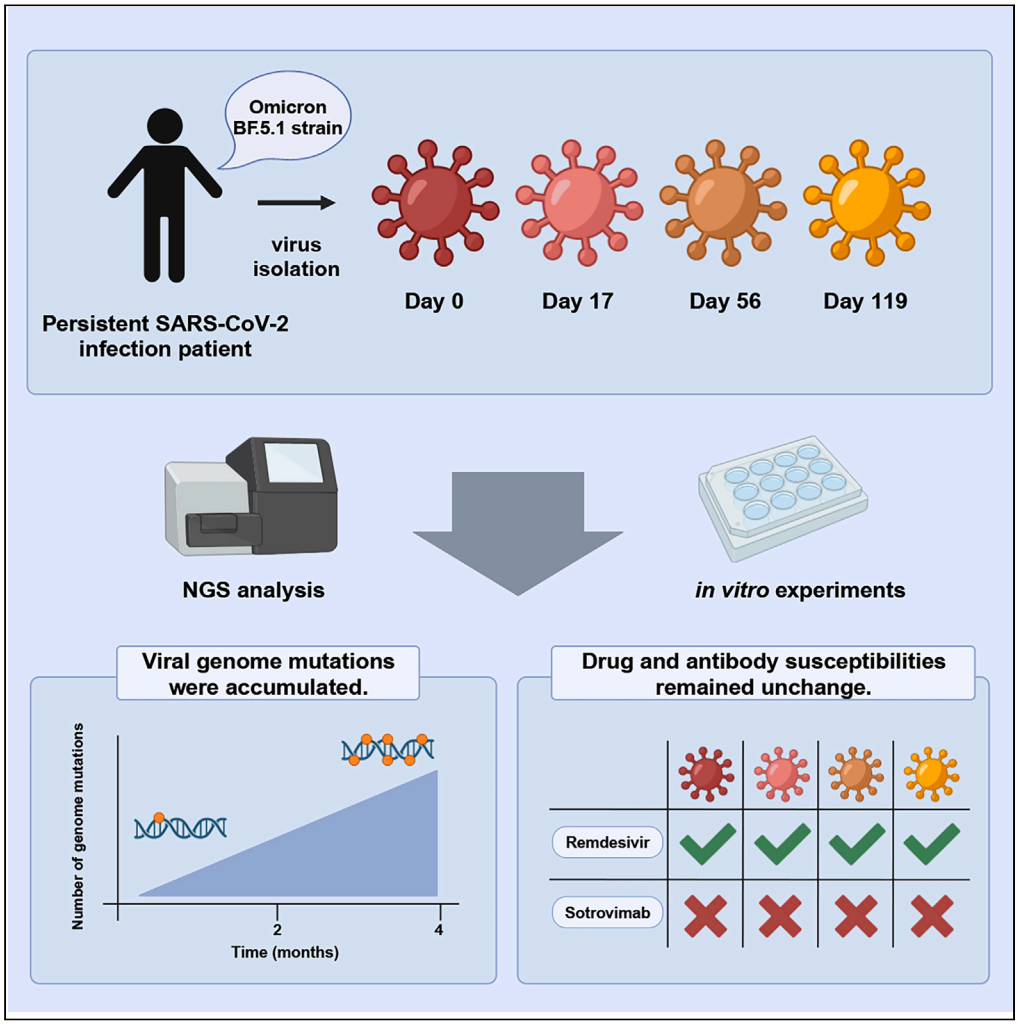

Hiroki Futatsusako, Rina Hashimoto, Masaki Yamamoto, ..., Kei Sato, Miki Nagao, Kazuo Takayama

mnagao@kuhp.kyoto-u.ac.jp (M.N.)
kazuo.takayama@cira.kyoto-u.ac.jp (K.T.)

Highlights

We isolated SARS-CoV-2 from a patient persistently infected with Omicron strain BF.5

Viral genome mutations were accumulated during the persistent SARS-CoV-2 infection

The susceptibility of isolates to remdesivir and sotrovimab remained unchanged

Acquired mutations in isolates were confirmed in subsequent mutant strains

Futatsusako et al., iScience 27, 109597
May 17, 2024
https://doi.org/10.1016/j.isci.2024.109597

iScience

CellPress
OPEN ACCESS

Article

Longitudinal analysis of genomic mutations in SARS-CoV-2 isolates from persistent COVID-19 patient

Hiroki Futatsusako,[1] Rina Hashimoto,[1] Masaki Yamamoto,[2] Jumpei Ito,[3,4,5] Yasufumi Matsumura,[2] Hajime Yoshifuji,[6] Kotaro Shirakawa,[7] Akifumi Takaori-Kondo,[7] The Genotype to Phenotype Japan (G2P-Japan) Consortium, Kei Sato,[3,4,5,8,9,10,11] Miki Nagao,[2,*] and Kazuo Takayama[1,12,13,*]

SUMMARY

A primary reason for the ongoing spread of coronavirus disease 2019 (COVID-19) is the continuous acquisition of mutations by the severe acute respiratory syndrome coronavirus 2 (SARS-CoV-2). However, the mechanism of acquiring mutations is not fully understood. In this study, we isolated SARS-CoV-2 from an immunocompromized patient persistently infected with Omicron strain BF.5 for approximately 4 months to analyze its genome and evaluate drug resistance. Although the patient was administered the antiviral drug remdesivir (RDV), there were no acquired mutations in RDV binding site, and all isolates exhibited susceptibility to RDV. Notably, upon analyzing the S protein sequence of the day 119 isolate, we identified mutations acquired by mutant strains emerging from the BF.5 variant, suggesting that viral genome analysis in persistent COVID-19 patients may be useful in predicting viral evolution. These results suggest mutations in SARS-CoV-2 are acquired during long-term viral replication rather than in response to antiviral drugs.

INTRODUCTION

Severe acute respiratory syndrome coronavirus 2 (SARS-CoV-2) has infected many people worldwide since it was first identified in Wuhan, China, in December 2019. A principal factor for its continued spread is believed to be its high mutation frequency that produces new variant strains. SARS-CoV-2 mutant strains differ not only in their pathogenicity and infectivity but also result in substantial differences in resistance to neutralizing antibodies.[1] Understanding the mechanisms by which mutant strains arise and predicting which mutant strains will become prevalent in the future are important challenges to tackle.

SARS-CoV-2 is known to acquire mutations through various processes, such as replication errors, viral recombination within the same host,[2] host RNA editing system,[3] and drug selection.[4,5] However, the main factors behind the emergence of mutant strains of SARS-CoV-2 remain unclear. In many coronavirus disease 2019 (COVID-19) patients, the virus is eliminated about a week after onset, making it difficult to observe the process by which the viral genome changes.[6] On the other hand, the process through which SARS-CoV-2 acquires mutations has been observed in immunocompromized patients susceptible to persistent SARS-CoV-2 infections.[7–12] Therefore, persistent COVID-19 patients are an optimal model for investigating the mechanisms by which mutant strains emerge. Additionally, analysis of persistent COVID-19 patients treated with antiviral drugs or antibodies can reveal the effects of these treatment options on the viral genome.

In this study, we performed analysis using samples from an immunocompromized patient persistently infected with COVID-19 for 4 months, during which antiviral drug, remdesivir (RDV), and anti-spike (S) protein antibody, sotrovimab, were administered. The genomic sequence of SARS-CoV-2 isolated from this patient was temporally analyzed using next-generation sequencing (NGS), and the viral replicability and drug resistance of the isolates were examined. While there have been several reports analyzing the evolution of the viral genome in patients with

[1]Center for iPS Cell Research and Application (CiRA), Kyoto University, Kyoto 6068507, Japan
[2]Department of Clinical Laboratory Medicine, Graduate School of Medicine, Kyoto University, Kyoto 6068507, Japan
[3]Division of Systems Virology, Department of Microbiology and Immunology, The Institute of Medical Science, The University of Tokyo, Tokyo 1088639, Japan
[4]Graduate School of Medicine, The University of Tokyo, Tokyo 1138654, Japan
[5]International Research Center for Infectious Diseases, The Institute of Medical Science, The University of Tokyo, Tokyo 1088639, Japan
[6]Department of Rheumatology and Clinical Immunology, Graduate School of Medicine, Kyoto University, Kyoto 6068507, Japan
[7]Department of Hematology, Graduate School of Medicine, Kyoto University, Kyoto 6068507, Japan
[8]International Vaccine Design Center, The Institute of Medical Science, The University of Tokyo, Tokyo 1088639, Japan
[9]Graduate School of Frontier Sciences, The University of Tokyo, Kashiwa 2770882, Japan
[10]Collaboration Unit for Infection, Joint Research Center for Human Retrovirus infection, Kumamoto University, Kumamoto 8600811, Japan
[11]CREST, Japan Science and Technology Agency, Kawaguchi 3320012, Japan
[12]AMED-CREST, Japan Agency for Medical Research and Development (AMED), Tokyo 1000004, Japan
[13]Lead contact
*Correspondence: mnagao@kuhp.kyoto-u.ac.jp (M.N.), kazuo.takayama@cira.kyoto-u.ac.jp (K.T.)
https://doi.org/10.1016/j.isci.2024.109597

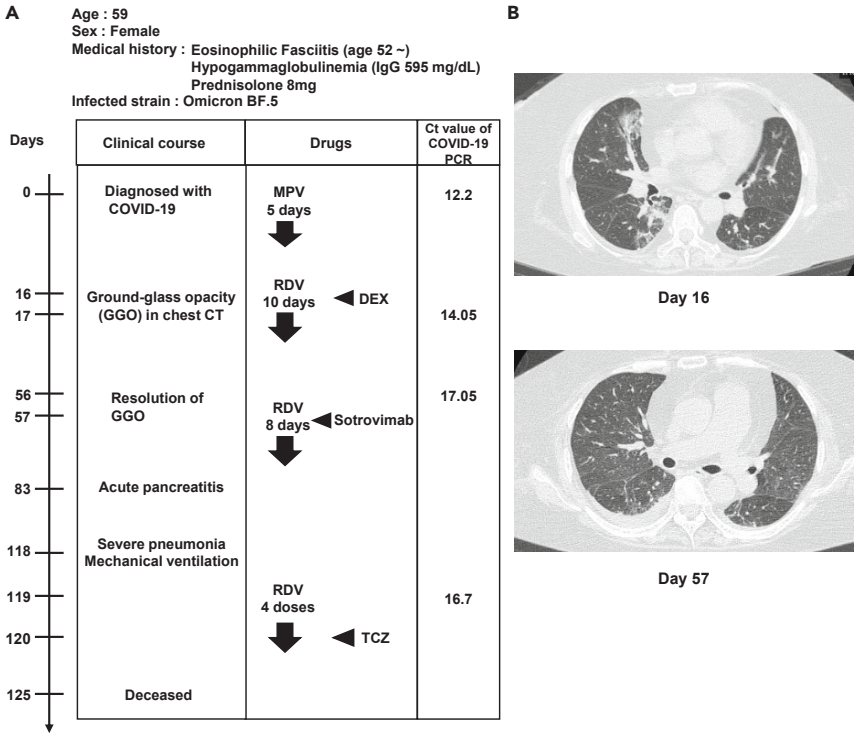

Figure 1. Profile of persistent COVID-19 patient

(A) Summary of the medical biography of the persistent coronavirus disease 2019 (COVID-19) patient. Diagnosis, drug administrations, and quantitative PCR (qPCR) cycle threshold values of patient nasopharyngeal swab specimens.

(B) Chest computed tomography (CT) images taken on days 16 and 57 after the disease onset. MPV, molnupiravir, RDV, remdesivir, DEX, dexamethasone, TCZ, tocilizumab.

persistent SARS-CoV-2 infection,[7–12] to the best of our knowledge, few studies have characterized viruses isolated from persistent COVID-19 patients to identify crucial factors involved in the emergence of mutant strains. These studies are expected to reveal at least part of the mechanism by which SARS-CoV-2 acquires mutations.

RESULTS

Profile of the persistent COVID-19 patient

The medical biography of the patient with persistent SARS-CoV-2 infection is summarized in Figure 1A. The patient was a 59-year-old woman with eosinophilic fasciitis and hypogammaglobulinemia. For treatment of eosinophilic fasciitis therapy, she had been prescribed prednisolone, an immunosuppressant, for approximately 8 years. The serum IgG concentration was 595 mg/dL before the administration. At day 48, intravenous immunoglobulin (IVIG) was administered, and the IgG concentration increased to the normal range (861–1,747 mg/dL). However, the IgG concentration decreased several days after IVIG administration, indicating that the patient was severely immunosuppressed. Following infection with the SARS-CoV-2 Omicron strain BF.5, this patient underwent periods of symptom remission and subsequent flare-ups, including pneumonia. Distinctive ground-glass opacifications, indicative of COVID-19 pneumonia, were observed in the chest computed tomography (CT) image on day 16 (Figure 1B, top); however, these opacities were notably absent on day 57 (Figure 1B, bottom). On day 83, the patient developed acute pancreatitis and severe pneumonia. Despite receiving artificial ventilation and tocilizumab (TCZ) treatment, the patient succumbed on day 125. PCR tests performed on days 0, 17, 56, and 119 detected a large amount of viral genome (Ct values = 12.2, 14.05, 17.05, and 16.7, respectively), indicating that the patient was infected with COVID-19 persistently.

Molnupiravir (MPV), remdesivir (RDV), and sotrovimab were used to treat this patient with persistent SARS-CoV-2 infection. The patient also received two doses of the COVID-19 vaccine. Swab specimens and serum were temporally collected from the patient with persistent SARS-CoV-2 infection at onset (day 0) and thereafter. Therefore, we considered this case optimal for investigating the causes of the emergent mutant strains.

Measurement of serum antibodies and cytokines in the patient with persistent SARS-CoV-2 infection

To comprehend the mechanisms underpinning the establishment of persistent infection in this patient, we measured the IgG antibody concentration against the receptor binding domain (RBD) of the S protein of SARS-CoV-2 in the patient's serum (Figure 2A). Antibody

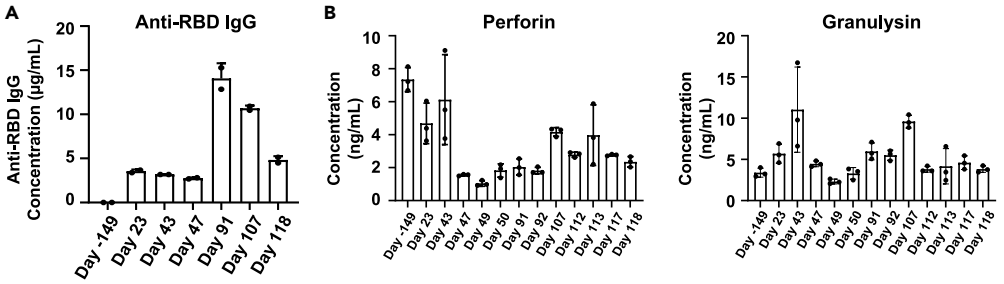

C

	IL-1β	IL-6	TNF-α	IP-10	IFN-λ1	IL-8	IL-12p70	IFN-α2	GM-CSF	IFN-β	IL-10	IFN-γ
Day -149	43.33	<7.80	<15.10	891.24	224.67	466.31	<4.10	<15.00	<4.40	215.47	<12.83	<204.72
Day 23	<27.56	17.51	<15.10	2255.27	<188.87	310.67	<4.10	<15.00	<4.40	<80.19	395.97	242.00
Day 50	<27.56	20.94	<15.10	860.88	<188.87	120.65	<4.10	<15.00	<4.40	89.14	49.33	<204.72
Day 91	<27.56	474.13	<15.10	2571.61	<188.87	1208.38	<4.10	<15.00	<4.40	<80.19	258.53	528.99
Day 92	<27.56	178.05	<15.10	1799.09	<188.87	851.95	<4.10	<15.00	<4.40	<80.19	399.37	2090.64
Day 107	100.24	128.42	46.40	931.37	356.87	1625.96	19.92	36.66	111.41	225.04	255.48	617.62
Day 118	30.24	88.41	15.13	917.20	197.12	427.24	5.19	<15.00	42.47	131.90	93.98	227.35

(pg/mL)

Detection limit Detected maximum value

Figure 2. Quantification of anti-RBD IgG antibody, cytolytic granules, and cytokine concentrations in the patient's serum

(A) Anti-receptor binding domain (RBD) IgG antibody concentration (μg/mL) in the patient's serum from day −149 (before COVID-19 diagnosis) to day 118 was measured by ELISA. Data are shown as mean ± SD (technical duplicates).

(B) Cytolytic granules (perforin, granulysin) concentration (pg/mL) in the patient's serum was measured by bead-based immunoassays. Data are shown as mean ± SD (n = 3).

(C) The concentration (pg/mL) of 12 types of inflammatory cytokines in the patient's serum was measured by bead-based immunoassays. Data are shown as means (n = 3).

concentration was below the detection limit (0.625 μg/mL or less) before onset (day −149) and remained around 3 μg/mL after onset. This value was lower than the median value (approximately 8 μg/mL) of people infected with COVID-19 one month after onset.[13] Antibody concentration increased transiently on days 91 and 107 because of sotrovimab administration on day 57. These results suggest the patient with persistent SARS-CoV-2 infection could not continuously produce antibodies against SARS-CoV-2, consistent with the observation that the virus was not eliminated from this patient.

It has been reported that natural killer (NK) cells and CD8-positive T cells contribute to virus clearance in COVID-19 patients.[14,15] When we measured the cytolytic granules in serum from this patient (Figure 2B), high concentrations of perforin and granulysin were detected, suggesting that NK cells and CD8-positive T cells are likely functional in this patient. However, the virus was not eliminated in this patient, suggesting NK cells and CD8-positive T cells alone are insufficient to eliminate the virus under conditions where there are almost no antibodies against the virus.

SARS-CoV-2 infection is known to cause a cytokine storm in severe COVID-19 cases.[16,17] Thus, we measured the concentrations of 12 inflammatory cytokines in the patient's serum (Figure 2C). Although most cytokine concentrations were low early during the infection, we detected increased concentrations of several cytokines known to be involved in the cytokine storm observed in severe COVID-19, including interleukin-6 (IL-6) and tumor necrosis factor-α (TNF-α),[16] after day 91. Therefore, while the virus was detected throughout the entire process of persistent SARS-CoV-2 infection, cytokine overproduction and symptom worsening occurred only during the latter infection stage. To identify the cause of worsening symptoms in persistent SARS-CoV-2 infection, it was necessary to analyze factors other than viral load.

Viral infectivity remained unchanged in isolates from the persistent COVID-19 patients

To investigate how SARS-CoV-2 evolved in the patient with persistent infection, we isolated the virus from swab samples collected on days 0, 17, 56, and 119 and performed NGS analysis (Figure 3A). The median tissue culture infectious dose (TCID50)/mL values of the four isolates were almost the same (Figure 3B), but the genomes of each isolate had different mutations (Figure 3C). While the genome mutated at 10 locations during days 0–17, the genome mutated at 27 and 37 locations during days 18–56 and 57–119, respectively. This result suggests that the virus may be more likely to acquire genomic mutations if infection extends beyond two months, and SARS-CoV-2 evolution could be tracked in this patient.

To examine the replication capacity of each isolate and its effects on host cells, human induced pluripotent stem (iPS) cell-derived lung organoids were infected with each isolate. Viral copy number in the culture supernatant was at almost the same level for each isolate

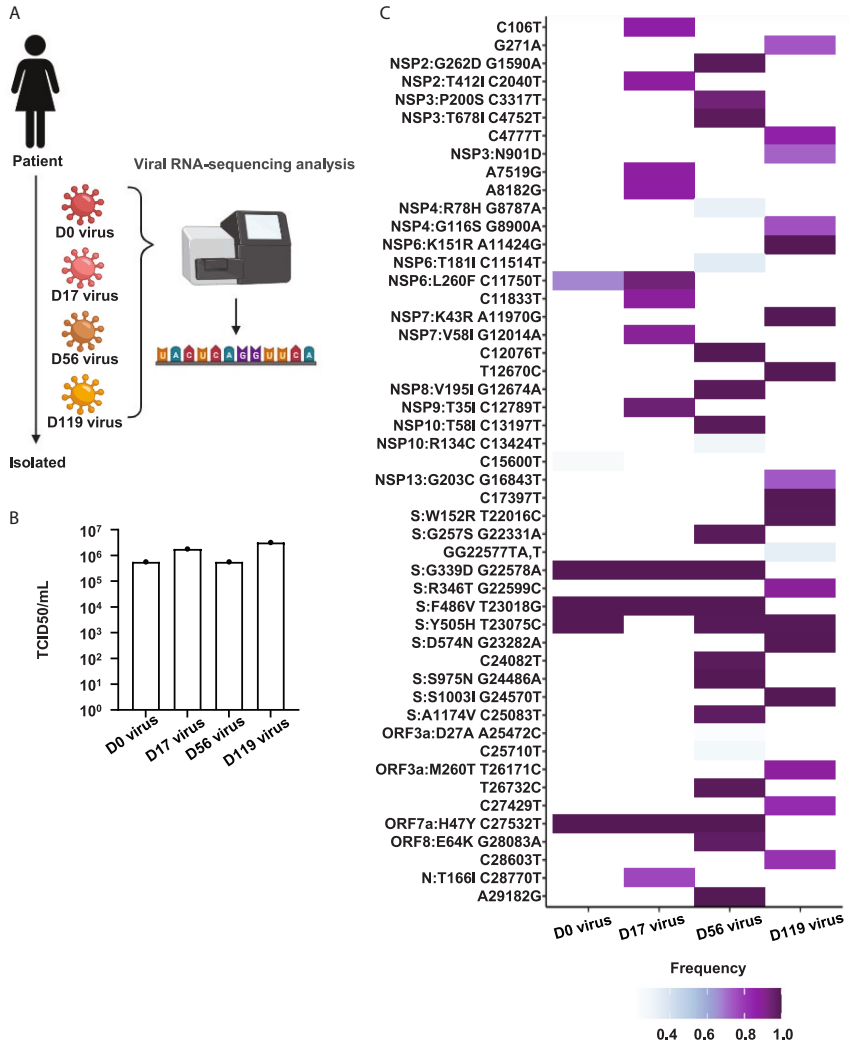

Figure 3. Genome analysis of isolated viruses

(A) Viruses were isolated from the patient swabs on days 0, 17, 56, and 119. Viral genome sequence was identified by next-generation sequencing (NGS analysis. Created with BioRender.com (https://www.biorender.com/).

(B) The amount of infectious virus in four isolate stocks were measured using the median tissue culture infectious dose (TCID50) assay.

(C) Heatmap of the viral genome variations compared with the Wuhan-Hu-1 reference sequence. Genome mutations detected in all viruses are not shown in this heatmap.

(Figure 4A). In addition, there were only minor differences in the mRNA expression of the SARS-CoV-2 nucleocapsid (N) in infected human iPS cell-derived lung organoids among isolates (Figure S1A). Expression of innate immune response-related genes significantly increased by infection with the day-17 isolate (Figure S1B), suggesting the day-17 isolate may have acquired mutations related to the induced expression of genes related to the innate immune response, thus warranting further analysis. Furthermore, expression of angiotensin-converting enzyme 2 (ACE2), critical for SARS-CoV-2 infection, was decreased by infection using all isolates (Figure S1C). These results suggest that the infectivity of the virus to human lung cells remains unchanged during persistent infection.

No new drug-resistant viruses emerged in the patient with persistent SARS-CoV-2 infection

We next investigated whether SARS-CoV-2 acquires resistance to therapeutic drugs during persistent infection. Using human iPS cell-derived lung organoids and the four isolates, we examined the sensitivity of isolates to the antiviral drug, RDV, and anti-spike (S) antibody, sotrovimab (Figures 4B and S2). All isolates had high susceptibility to RDV (half maximal effective concentration (EC50) = 6–90 nM) but low susceptibility to sotrovimab (EC50 > 10 mg/mL). Analysis of the S protein sequences revealed that all isolated viruses had genomic mutations (G339D or R346T)[18–20] that are known to be related to resistance to sotrovimab (Figures 4C and S3), consistent with the isolates showing resistance to sotrovimab. Furthermore, mutations in non-structural protein (NSP)12 involved in the acquisition of RDV resistance[5,21] were not identified

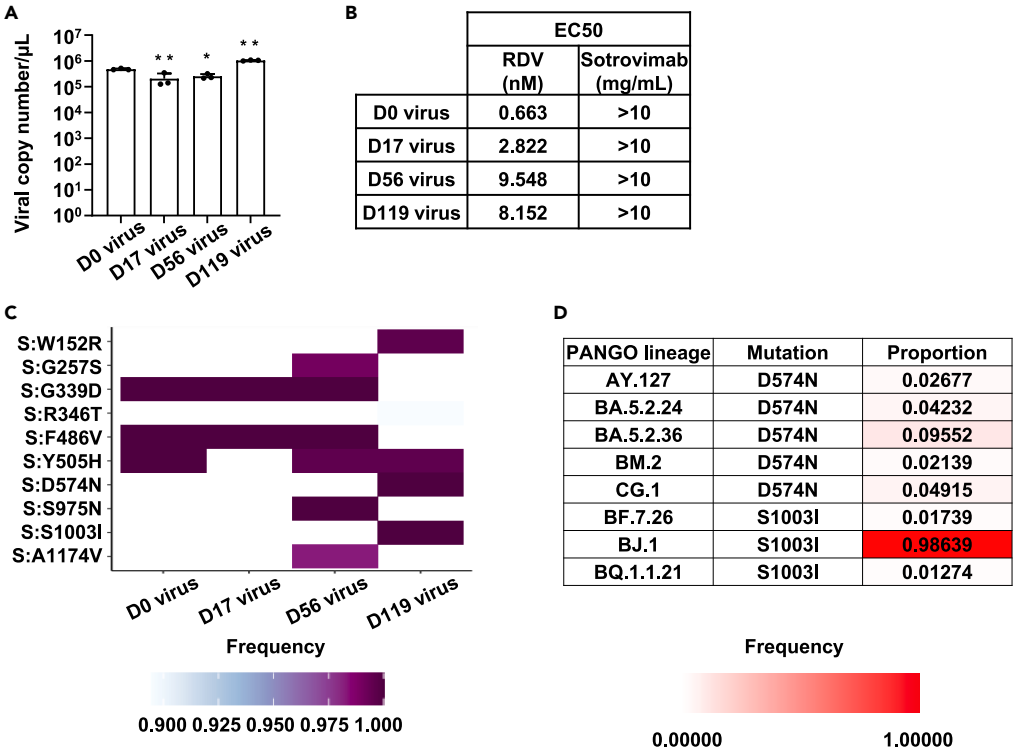

Figure 4. Sensitivity of isolated viruses to antiviral drugs and antibodies

(A) Human induced pluripotent stem (iPS) cell-derived lung organoids were infected with a 0.1 multiplicity of infection (MOI) of isolated viruses and cultured for 4 days. Viral RNA copy number in the cell culture supernatant as measured by qPCR. Statistical significance between day 0 virus and other isolated viruses was determined by one-way analysis of variance (ANOVA) followed by Dunnett post hoc tests (*$p < 0.05$, **$p < 0.01$). Data are shown as mean ± SD ($n = 3$).

(B) Human iPS cell-derived lung organoids were infected with 0.1 MOI of isolated viruses in the presence MOI or absence of remdesivir (RDV) or sotrovimab and cultured for 4 days. Viral RNA copy number in the cell culture supernatant as measured by qPCR. The EC50 of remdesivir or sotrovimab was determined.

(C) Heatmap of the spike genome variations compared with the Wuhan-Hu-1 reference sequence. Genome mutations detected in all viruses are not shown.

(D) SARS-CoV-2 variants with D574N or S1003I are summarized. The variant proportion with these mutations in each lineage. See also Figures S1–S3.

in any viral isolate (Figure 3C). These results suggest that susceptibility to antiviral drugs and antibodies does not change during persistent infection.

Predicting viral evolution in the patient with persistent SARS-CoV-2 infection

We investigated whether it would be possible to predict viral evolution by analyzing the virus isolated from the patient with persistent SARS-CoV-2 infection. In this analysis, we focused on the S protein amino acid sequence (Figures 4C and S3). Mutations, W152R and G257S, acquired by the virus during persistent infection, are frequently observed in BA.2.75 strain,[22] which is phylogenetically different from the BF.5 strain. D574N, S975N, S1003I, and A1174V, acquired while the patient was persistently infected with the BF.5 strain, are mutations that have rarely been reported before the appearance of this strain. Thus, we determined the frequency of these four mutations in the mutant strains after the appearance of BF.5. Importantly, D574N and S1003I were found in more than 1% of the descendant strains of BA.5 (BA.5.24, BA.5.2.36, CG.1, BF.7.26, and BQ.1.1.21). Furthermore, D574N and S1003I were also confirmed in mutant strains that are phylogenetically different from BF.5, such as AY.127, BM.2, and BJ.1 (Figure 4D). These results suggest that the BF.5 strain had acquired the mutations, which can be observed in the mutant strains that appeared after the BF.5 strain, during the approximately four-month period of persistent infection. These findings highlight the potential to forecast the virus' evolution by analyzing it in patients with persistent SARS-CoV-2 infection. On the other hand, S975N and A1174V were hardly detected in other mutant strains, thus suggesting some genome mutations may not be related to virus evolution in the real world.

DISCUSSION

In this study, we analyzed the evolution of the virus using samples from a patient with persistent SARS-CoV-2 infection. Our analysis suggests a low likelihood of drug-resistant viruses emerging due to drug administration. Instead, it indicates a higher probability of the virus acquiring mutations following persistent infections lasting over two months or more. In the future, it is expected that by examining the patterns in which mutations appear, it would be possible to predict the mutations of future mutant strains.

Several reports have suggested RDV-resistant mutations appear due to RDV administration.[5,11,21] Despite the long-term RDV use involved in this study (Figure 1A), viral isolates remained highly susceptible to RDV (Figures 3C, 4B, and S2A). These results suggest that the selective pressure of drug administration is not necessarily involved in the acquisition of drug-resistant mutations. However, since this study only analyzed one patient with persistent SARS-CoV-2 infection, it will be necessary to examine more patients with persistent SARS-CoV-2 infection to confirm the generality of this observation. Furthermore, although this patient's virus remained susceptible to RDV, RDV administration alone was unable to eliminate the virus, suggesting that the combination and administration period of antiviral drugs for the treatment of patients with persistent SARS-CoV-2 infection can be further optimized.

Limitations of the study

In this study, we identified genomic mutations by NGS analysis of isolates. However, it should be noted that we performed a short-read NGS analysis, so it is impossible to conduct a precise analysis if two or more mutant strains are present in the patient with persistent SARS-CoV-2 infection. To analyze the virus genome more accurately, long-read NGS analysis is necessary in the future. This study has another limitation in that it relies on a single case, constraining the rationale for generalizing how viral genomic analysis of persistent COVID-19 cases might contribute to predicting viral evolution. Furthermore, it is also essential to clarify the functions of the identified genomic mutations. We have evaluated the impact of genomic mutations on virological characteristics through a combination of *in vitro* respiratory models, like airway organoids and airway-on-a-chip, and *in vivo* models, including hamsters. These approaches have consistently unveiled distinctive traits of mutant strains,[2,23–26] thus together comprise a toolbox of great utility in analyzing mutant strains obtained from persistent COVID-19 patients.

CONSORTIUM

We thank Keita Matsuno, Naganori Nao, Hirofumi Sawa, Shinya Tanaka, Masumi Tsuda, Lei Wang, Yoshikata Oda, Zannatul Ferdous, Kenji Shishido, Takasuke Fukuhara, Tomokazu Tamura, Rigel Suzuki, Saori Suzuki, Shuhei Tsujino, Hayato Ito, Yu Kaku, Naoko Misawa, Arnon Plianchaisuk, Ziyi Guo, Alfredo, Jr. Amolong Hinay, Kaoru Usui, Wilaiporn Saikruang, Keiya Uriu, Yusuke Kosugi, Shigeru Fujita, Jarel Elgin Mendoza Tolentino, Luo Chen, Lin Pan, Mai Suganami, Mika Chiba, Ryo Yoshimura, Kyoko Yasuda, Keiko Iida, Adam Patrick Strange, Naomi Ohsumi, Shiho Tanaka, Kaho Okumura, Kazuhisa Yoshimura, Kenji Sadamasu, Mami Nagashima, Hiroyuki Asakura, Isao Yoshida, So Nakagawa, Kayoko Nagata, Ryosuke Nomura, Yoshihito Horisawa, Yusuke Tashiro, Yugo Kawai, Sayaka Deguchi, Yukio Watanabe, Yoshitaka Nakata, Ayaka Sakamoto, Naoko Yasuhara, Takao Hashiguchi, Tateki Suzuki, Kanako Kimura, Jiei Sasaki, Yukari Nakajima, Hisano Yajima, Takashi Irie, Ryoko Kawabata, Kaori Tabata, Terumasa Ikeda, Hesham Nasser, Ryo Shimizu, MST Monira Begum, Michael Jonathan, Yuka Mugita, Sharee Leong, Otowa Takahashi, Kimiko Ichihara, Takamasa Ueno, Chihiro Motozono, Mako Toyoda, Akatsuki Saito, Maya Shofa, Yuki Shibatani, Tomoko Nishiuchi, Jiri Zahradnik, Prokopios Andrikopoulos, Miguel Padilla Blanco, and Aditi Konar as the member of The Genotype to Phenotype Japan (G2P-Japan) Consortium.

STAR★METHODS

Detailed methods are provided in the online version of this paper and include the following:

- KEY RESOURCES TABLE
- RESOURCE AVAILABILITY
  - Lead contact
  - Materials availability
  - Data and code availability
- EXPERIMENTAL MODEL AND STUDY PARTICIPANT DETAILS
  - COVID-19 patient samples
  - Human iPS cells
  - Human iPS cell-derived lung organoids
- METHOD DETAILS
  - SARS-CoV-2 isolation
  - SARS-CoV-2 genome analysis
  - SARS-CoV-2 titration
  - Quantification of viral RNA copy number
  - Antiviral drug/antibody assay using SARS-CoV-2 isolates and human iPS cell-derived lung organoids
  - RT-qPCR
  - Measurement of the concentration of IgG antibody against SARS-CoV-2 S-RBD
  - Measurement of cytokines in serum
- QUANTIFICATION AND STATISTICAL ANALYSIS

SUPPLEMENTAL INFORMATION

Supplemental information can be found online at https://doi.org/10.1016/j.isci.2024.109597.

ACKNOWLEDGMENTS

We thank Dr. Kelvin Hui (Kyoto University) for critical reading of the manuscript, Dr. Yoshio Koyanagi, Dr. Takeshi Noda, Dr. Kazuya Shimura, and Dr. Yukiko Muramoto (Kyoto University) for setup and operation of the BSL-3 laboratory at Kyoto University, and Ms. Ayaka Sakamoto, Ms. Naoko Yasuhara, and Ms. Natsumi Mimura (Kyoto University) for technical assistance. Graphical abstract was created with BioRender.com (https://www.biorender.com/).

This work was supported by the iPS Cell Research Fund, the COVID-19 Private Fund (to the Shinya Yamanaka laboratory, CiRA, Kyoto University), and the Japan Agency for Medical Research and Development (AMED) (grant numbers JP21gm1610005, JP22fk0108511, JP23jf0126002).

AUTHOR CONTRIBUTIONS

H.F. analyzed samples obtained from the immunocompromized patient and wrote the manuscript. R.H. performed the SARS-CoV-2 infection experiments. M.Y. collected the clinical samples. J.I. performed NGS analysis. Y.M. collected the clinical samples and performed NGS analysis, H.Y., K.S., and A.T. collected the clinical samples. K.S. designed the study. M.N. collected the clinical samples and designed the study. K.T. conceived and designed the study, analyzed and interpreted the data, and wrote the manuscript.

DECLARATION OF INTERESTS

J.I. has consulting fees and honoraria for lectures from Takeda Pharmaceutical Co. Ltd. K.S. has consulting fees from Moderna Japan Co., Ltd. and Takeda Pharmaceutical Co. Ltd. and honoraria for lectures from Gilead Sciences, Inc., Moderna Japan Co., Ltd., and Shionogi & Co., Ltd.

Received: January 19, 2024
Revised: February 20, 2024
Accepted: March 25, 2024
Published: March 29, 2024

REFERENCES

1. Carabelli, A.M., Peacock, T.P., Thorne, L.G., Harvey, W.T., Hughes, J., COVID-19 Genomics UK Consortium, Peacock, S.J., Barclay, W.S., de Silva, T.I., Towers, G.J., and Robertson, D.L. (2023). SARS-CoV-2 variant biology: immune escape, transmission and fitness. Nat. Rev. Microbiol. *21*, 162–177. https://doi.org/10.1038/s41579-022-00841-7.
2. Tamura, T., Ito, J., Uriu, K., Zahradnik, J., Kida, I., Anraku, Y., Nasser, H., Shofa, M., Oda, Y., Lytras, S., et al. (2023). Virological characteristics of the SARS-CoV-2 XBB variant derived from recombination of two Omicron subvariants. Nat. Commun. *14*, 2800. https://doi.org/10.1038/s41467-023-38435-3.
3. Harris, R.S., and Dudley, J.P. (2015). APOBECs and virus restriction. Virology *479–480*, 131–145. https://doi.org/10.1016/j.virol.2015.03.012.
4. Gordon, C.J., Tchesnokov, E.P., Schinazi, R.F., and Götte, M. (2021). Molnupiravir promotes SARS-CoV-2 mutagenesis via the RNA template. J. Biol. Chem. *297*, 100770. https://doi.org/10.1016/j.jbc.2021.100770.
5. Hogan, J.I., Duerr, R., Dimartino, D., Marier, C., Hochman, S.E., Mehta, S., Wang, G., and Heguy, A. (2023). Remdesivir Resistance in Transplant Recipients With Persistent Coronavirus Disease 2019. Clin. Infect. Dis. *76*, 342–345. https://doi.org/10.1093/cid/ciac769.
6. Cevik, M., Kuppalli, K., Kindrachuk, J., and Peiris, M. (2020). Virology, transmission, and pathogenesis of SARS-CoV-2. BMJ *371*, m3862. https://doi.org/10.1136/bmj.m3862.
7. Cele, S., Karim, F., Lustig, G., San, J.E., Hermanus, T., Tegally, H., Snyman, J., Moyo-Gwete, T., Wilkinson, E., Bernstein, M., et al. (2022). SARS-CoV-2 prolonged infection during advanced HIV disease evolves extensive immune escape. Cell Host Microbe *30*, 154–162.e5. https://doi.org/10.1016/j.chom.2022.01.005.
8. Mazzetti, P., Spezia, P.G., Capria, A.L., Freer, G., Sidoti, M., Costarelli, S., Cara, A., Rosellini, A., Frateschi, S., Moscato, G., et al. (2023). SARS-CoV-2 evolution during persistent infection in a CAR-T recipient shows an escape to both sotrovimab and T-cell responses. J. Clin. Virol. *3*, 100149. https://doi.org/10.1016/j.jcvp.2023.100149.
9. Kaya, H., Tani, H., Inasaki, N., Yazawa, S., Itamochi, M., Higashi, D., Tsuji, N., Nakamura, M., and Oishi, K. (2023). Virus evolution and reduced viral viability during treatment of persistent COVID-19 Omicron BA.5 infection in an immunocompromised host. Int. J. Infect. Dis. *136*, 146–148. https://doi.org/10.1016/j.ijid.2023.09.010.
10. Hettle, D., Hutchings, S., Muir, P., and Moran, E.; COVID-19 Genomics UK COG-UK consortium (2022). Persistent SARS-CoV-2 infection in immunocompromised patients facilitates rapid viral evolution: Retrospective cohort study and literature review. Clin. Infect. Pract. *16*, 100210. https://doi.org/10.1016/j.clinpr.2022.100210.
11. Hirotsu, Y., Kobayashi, H., Kakizaki, Y., Saito, A., Tsutsui, T., Kawaguchi, M., Shimamura, S., Hata, K., Hanawa, S., Toyama, J., et al. (2023). Multidrug-resistant mutations to antiviral and antibody therapy in an immunocompromised patient infected with SARS-CoV-2. Méd. *4*, 813–824.e4. https://doi.org/10.1016/j.medj.2023.08.001.
12. Halfmann, P.J., Minor, N.R., Haddock Iii, L.A., Maddox, R., Moreno, G.K., Braun, K.M., Baker, D.A., Riemersa, K.K., Prasad, A., Alman, K.J., et al. (2023). Evolution of a globally unique SARS-CoV-2 Spike E484T monoclonal antibody escape mutation in a persistently infected, immunocompromised individual. Virus Evol. *9*, veac104. https://doi.org/10.1093/ve/veac104.
13. Zhan, Y., Zhu, Y., Wang, S., Jia, S., Gao, Y., Lu, Y., Zhou, C., Liang, R., Sun, D., Wang, X., et al. (2021). SARS-CoV-2 immunity and functional recovery of COVID-19 patients 1-year after infection. Signal Transduct. Targeted Ther. *6*, 368. https://doi.org/10.1038/s41392-021-00777-z.
14. Dizaji Asl, K., Mazloumi, Z., Majidi, G., Kalarestaghi, H., Sabetkam, S., and Rafat, A. (2022). NK cell dysfunction is linked with disease severity in SARS-CoV-2 patients. Cell Biochem. Funct. *40*, 559–568. https://doi.org/10.1002/cbf.3725.
15. Rahman, M.D.T., Ryu, S., Achangwa, C., Hwang, J.H., Hwang, J.H., and Lee, C.S. (2023). Temporal Dynamics of Serum Perforin and Granzyme during the Acute Phase of SARS-CoV-2 Infection. Vaccines *11*, 1314. https://doi.org/10.3390/vaccines11081314.
16. Hu, B., Huang, S., and Yin, L. (2021). The cytokine storm and COVID-19. J. Med. Virol. *93*, 250–256. https://doi.org/10.1002/jmv.26232.
17. Ye, Q., Wang, B., and Mao, J. (2020). The pathogenesis and treatment of the 'Cytokine Storm' in COVID-19. J. Infect. *80*, 607–613. https://doi.org/10.1016/j.jinf.2020.03.037.
18. Jawad, B., Adhikari, P., Podgornik, R., and Ching, W.Y. (2022). Binding Interactions between Receptor-Binding Domain of Spike Protein and Human Angiotensin Converting Enzyme-2 in Omicron Variant. J. Phys. Chem. Lett. *13*, 3915–3921. https://doi.org/10.1021/acs.jpclett.2c00423.
19. Cao, Y., Wang, J., Jian, F., Xiao, T., Song, W., Yisimayi, A., Huang, W., Li, Q., Wang, P., An, R., et al. (2022). Omicron escapes the majority of existing SARS-CoV-2 neutralizing antibodies. Nature *602*, 657–663. https://doi.org/10.1038/s41586-021-04385-3.

20. Andrés, C., González-Sánchez, A., Jiménez, M., Márquez-Algaba, E., Piñana, M., Fernández-Naval, C., Esperalba, J., Saubi, N., Quer, J., Rando-Segura, A., et al. (2023). Emergence of Delta and Omicron variants carrying resistance-associated mutations in immunocompromised patients undergoing sotrovimab treatment with long-term viral excretion. Clin. Microbiol. Infect. *29*, 240–246. https://doi.org/10.1016/j.cmi.2022.08.021.
21. Torii, S., Kim, K.S., Koseki, J., Suzuki, R., Iwanami, S., Fujita, Y., Jeong, Y.D., Ito, J., Asakura, H., Nagashima, M., et al. (2023). Increased flexibility of the SARS-CoV-2 RNA-binding site causes resistance to remdesivir. PLoS Pathog. *19*, e1011231. https://doi.org/10.1371/journal.ppat.1011231.
22. Zhang, M., Chen, Z., Zhou, J., Zhao, X., Chen, Y., Sun, Y., Liu, Z., Gu, W., Luo, C., Fu, X., and Zhao, X. (2022). An imported human case with the SARS-CoV-2 Omicron subvariant BA.2.75 in Yunnan Province, China. Biosaf. Health *4*, 406–409. https://doi.org/10.1016/j.bsheal.2022.10.003.
23. Hashimoto, R., Tamura, T., Watanabe, Y., Sakamoto, A., Yasuhara, N., Ito, H., Nakano, M., Fuse, H., Ohta, A., Noda, T., et al. (2023). Evaluation of Broad Anti-Coronavirus Activity of Autophagy-Related Compounds Using Human Airway Organoids. Mol. Pharm. *20*, 2276–2287. https://doi.org/10.1021/acs.molpharmaceut.3c00114.
24. Hashimoto, R., Takahashi, J., Shirakura, K., Funatsu, R., Kosugi, K., Deguchi, S., Yamamoto, M., Tsunoda, Y., Morita, M., Muraoka, K., et al. (2022). SARS-CoV-2 disrupts respiratory vascular barriers by suppressing Claudin-5 expression. Sci. Adv. *8*, eabo6783. https://doi.org/10.1126/sciadv.abo6783.
25. Sano, E., Suzuki, T., Hashimoto, R., Itoh, Y., Sakamoto, A., Sakai, Y., Saito, A., Okuzaki, D., Motooka, D., Muramoto, Y., et al. (2022). Cell response analysis in SARS-CoV-2 infected bronchial organoids. Commun. Biol. *5*, 516. https://doi.org/10.1038/s42003-022-03499-2.
26. Saito, A., Tamura, T., Zahradnik, J., Deguchi, S., Tabata, K., Anraku, Y., Kimura, I., Ito, J., Yamasoba, D., Nasser, H., et al. (2022). Virological characteristics of the SARS-CoV-2 Omicron BA.2.75 variant. Cell Host Microbe *30*, 1540–1555.e15. https://doi.org/10.1016/j.chom.2022.10.003.
27. Matsuyama, S., Nao, N., Shirato, K., Kawase, M., Saito, S., Takayama, I., Nagata, N., Sekizuka, T., Katoh, H., Kato, F., et al. (2020). Enhanced isolation of SARS-CoV-2 by TMPRSS2-expressing cells. Proc. Natl. Acad. Sci. USA *117*, 7001–7003. https://doi.org/10.1073/pnas.2002589117.
28. Chen, S., Zhou, Y., Chen, Y., and Gu, J. (2018). fastp: an ultra-fast all-in-one FASTQ preprocessor. Bioinformatics *34*, i884–i890. https://doi.org/10.1093/bioinformatics/bty560.
29. Li, H., and Durbin, R. (2009). Fast and accurate short read alignment with Burrows-Wheeler transform. Bioinformatics *25*, 1754–1760. https://doi.org/10.1093/bioinformatics/btp324.
30. Li, H., Handsaker, B., Wysoker, A., Fennell, T., Ruan, J., Homer, N., Marth, G., Abecasis, G., and Durbin, R.; 1000 Genome Project Data Processing Subgroup (2009). The Sequence Alignment/Map format and SAMtools. Bioinformatics *25*, 2078–2079. https://doi.org/10.1093/bioinformatics/btp352.
31. Cingolani, P., Platts, A., Wang, L.L., Coon, M., Nguyen, T., Wang, L., Land, S.J., Lu, X., and Ruden, D.M. (2012). A program for annotating and predicting the effects of single nucleotide polymorphisms, SnpEff: SNPs in the genome of Drosophila melanogaster strain w1118; iso-2; iso-3. Fly *6*, 80–92. https://doi.org/10.4161/fly.19695.
32. Kimura, I., Yamasoba, D., Tamura, T., Nao, N., Suzuki, T., Oda, Y., Mitoma, S., Ito, J., Nasser, H., Zahradnik, J., et al. (2022). Virological characteristics of the SARS-CoV-2 Omicron BA.2 subvariants, including BA.4 and BA.5. Cell *185*, 3992–4007.e16. https://doi.org/10.1016/j.cell.2022.09.018.

STAR★METHODS

KEY RESOURCES TABLE

REAGENT or RESOURCE	SOURCE	IDENTIFIER
Bacterial and virus strains		
SARS-CoV-2 isolate (D0, strain BF.5, EPI_ISL_18909991)	This paper	N/A
SARS-CoV-2 isolate (D17, strain BF.5, EPI_ISL_18910061)	This paper	N/A
SARS-CoV-2 isolate (D56, strain BF.5, EPI_ISL_18910100)	This paper	N/A
SARS-CoV-2 isolate (D119, strain BF.5, EPI_ISL_18910101)	This paper	N/A
Biological samples		
Swab specimens from the COVID-19 patient	Kyoto University	N/A
Sera from the COVID-19 patient	Kyoto University	N/A
Chemicals, peptides, and recombinant proteins		
Eagle's Minimum Essential Media	FUJIFILM Wako Pure Chemical	Cat# 051-07615
TrypLE Select Enzyme	Thermo Fisher Scientific	Cat# 12563029
Human laminin 511 E8 fragments (iMatrix-511)	Nippi	Cat# 892 012
StemFit AK02N medium	Ajinomoto Healthy Supply	Cat# RCAK02N
Matrigel® Growth Factor Reduced Basement Membrane	Corning	Cat# 354230
D-MEM (High Glucose) with L-Glutamine and Phenol Red	FUJIFILM Wako Pure Chemical	Cat# 044-29765
DMEM/F-12	Thermo Fisher Scientific	Cat# 11320033
N2	FUJIFILM Wako Pure Chemical	Cat# 141-08941
B-27 Supplement Minus Vitamin A	Thermo Fisher Scientific	Cat# 12587001
Ascorbic acid	STEMCELL Technologies	Cat# ST-72132
GlutaMAX	Thermo Fisher Scientific	Cat# 35050-061
Monothioglycerol	FUJIFILM Wako Pure Chemical	Cat# 195-15791
Bovine serum albumin	Sigma-Aldrich	Cat# 820024
Y-27632	FUJIFILM Wako Pure Chemical	Cat# 034-24024
Recombinant Activin A	R&D Systems	Cat# 338-AC-01M
Dorsomorphin dihydrochloride	FUJIFILM Wako Pure Chemical	Cat# 047-33763
SB431542	FUJIFILM Wako Pure Chemical	Cat# 037-24293
IWP2	Stemolecule	Cat# 04-0034
CHIR99021	FUJIFILM Wako Pure Chemical	Cat# 034-23103
Human FGF10	PeproTech	Cat# AF-100-26
Human FGF7	PeproTech	Cat# AF-100-19
Human BMP4	PeproTech	Cat# 120-05ET
Human EGF	PeproTech	Cat# AF-100-15
All-trans retinoic acid	Sigma-Aldrich	Cat# R2625
Dexamethasone	Selleck Chemicals	Cat# S1322
8-bromo-cAMP	Tocris Bioscience	Cat# 1140/50
IBMX (3-isobutyl-1-methylxanthine)	FUJIFILM Wako Pure Chemical	Cat# 095-03413
SUPERase I™ RNase Inhibitor	Thermo Fisher Scientific	Cat# AM2696
Triton X-100	Nacalai Tesque	Cat# 35501-15
KCl	Nacalai Tesque	Cat# 13091-75
Tris-HCl (pH 7.5)	NIPPON GENE	Cat# 318-90225
Glycerol	Nacalai Tesque	Cat# 17017-93

(*Continued on next page*)

Continued

REAGENT or RESOURCE	SOURCE	IDENTIFIER
Remdesivir	Clinisciences	Cat# A17170
Sotrovimab	MedChemExpress	Cat# HY-P99340
ISOGENE	NIPPON GENE	Cat# 319-90211
SYBR Green PCR Master Mix	Thermo Fisher Scientific	Cat# 4385614
Critical commercial assays		
QIAamp viral RNA mini kit	Qiagen	Cat# 52906
NEBNext Ultra RNA Library Prep Kit for Illumina	New England Biolabs	Cat# E7530
MiSeq reagent kit v3	Illumina	Cat# MS-102-3001
One Step TB Green PrimeScript PLUS RT-PCR Kit (Perfect Real Time)	Takara Bio	Cat# RR096A
Superscript VILO cDNA Synthesis Kit	Thermo Fisher Scientific	Cat# 11754250
Anti-SARS-CoV-2 S-RBD protein Human IgG ELISA Kit	Proteintech	Cat# KE30003
Human Anti-Virus Response Panel	BioLegend	Cat# 740349
Human CD8/NK Panel	BioLegend	Cat #740267
Deposited data		
Viral genome sequencing data of isolate from swab samples collected on day 0	This paper	EPI_ISL_18909991
Viral genome sequencing data of isolate from swab samples collected on day 17	This paper	EPI_ISL_18910061
Viral genome sequencing data of isolate from swab samples collected on day 56	This paper	EPI_ISL_18910100
Viral genome sequencing data of isolate from swab samples collected on day 119	This paper	EPI_ISL_18910101
Experimental models: Cell lines		
African green monkey (*Chlorocebus sabaeus*): TMPRSS2/Vero cells	JCRB Cell Bank (Matsuyama et al.[27]	Cat# JCRB1818
Human: iPS cells (1383D6)	provided by Dr. Masato Nakagawa, Kyoto University	N/A
Oligonucleotides		
Primers and probes used for the quantification of viral RNA copy number, see Table S1	This paper	N/A
Primers used for RT-qPCR, see Table S2	This paper	N/A
Software and algorithms		
fastp v0.21.0	Chen et al.[28]	https://github.com/OpenGene/fastp
BWA-MEM v0.7.17	Lin and Durbin et al.[29]	http://bio-bwa.sourceforge.net
SAMtools v1.9	Li et al.[30]	http://www.htslib.org
snpEff v5.0e	Cingolani e al.[31]	http://pcingola.github.io/SnpEff
Prism 9 software v9.1.1	GraphPad Software	https://www.graphpad.com/scientific-software/prism/
Other		
96-well cell culture plates	Thermo Fisher Scientific	Cat# 167008
QuantStudio 1 real-time PCR system	Thermo Fisher Scientific	N/A
QuantStudio 3 real-time PCR system	Thermo Fisher Scientific	N/A
StepOnePlus real-time PCR system	Thermo Fisher Scientific	N/A
Multiskan FC	Thermo Fisher Scientific	N/A
MACSQuant Analyzer 10 Flow Cytometer	Milteniyi Biotec	N/A

RESOURCE AVAILABILITY

Lead contact

Further information and requests for resources and reagents should be directed to and will be fulfilled by the lead contact, Kazuo Takayama (kazuo.takayama@cira.kyoto-u.ac.jp).

Materials availability

All unique reagents generated in this study are listed in the key resources table and available from the lead contact with a completed Materials Transfer Agreement.

Data and code availability

- Data: All viral sequences used in this study are available from the GISAID database (https://www.gisaid.org). Accession ID is listed in the key resources table.
- Code: Not applicable.
- Any additional information required to reanalyze the data reported in this work is available from the lead contact upon request.

EXPERIMENTAL MODEL AND STUDY PARTICIPANT DETAILS

COVID-19 patient samples

The current study was performed in accordance with the Declaration of Helsinki and conducted with approval by the ethics committee of the Kyoto University Graduate School and Faculty of Medicine (R2379-3). Informed consent was obtained via an opt-out form on the institution's website. The institutional ethics committee approved this informed consent plan. Archived residual serum samples from patients with COVID-19 referred to Kyoto University Hospital, Kyoto, Japan, were used in this study. These clinical specimens were previously archived for future studies to identify novel biomarkers for disease progression but were repurposed for the present study. Patient information is summarized in Figure 1A.

Human iPS cells

The human induced pluripotent stem (iPS) cell lines, 1383D6 (provided by Dr. Masato Nakagawa, Kyoto University) were maintained on 0.5 μg/cm^2 recombinant human laminin 511 E8 fragments (iMatrix-511, Cat# 892 012, Nippi) with StemFit AK02N medium (Cat# RCAK02N, Ajinomoto Healthy Supply). Cell passage was performed every 6 days. For passaging, human iPS cell colonies were treated with TrypLE Select Enzyme (Cat# 12563029, Thermo Fisher Scientific) for 10 min at 37°C and seeded with StemFit AK02N medium containing 10 μM Y-27632 (Cat# 034–24024, FUJIFILM Wako Pure Chemical).

Human iPS cell-derived lung organoids

To start differentiation, human iPS cell colonies were treated with TrypLE Select Enzyme for 10 min at 37°C. After centrifugation, cells were seeded onto Matrigel Growth Factor Reduced Basement Membrane (Cat# 354230, Corning)-coated cell culture plates (2.0×10^5 cells/4 cm^2) and cultured for 2 days. The differentiation was performed in serum-free differentiation (SFD) medium of DMEM/F12 (3:1) (Cat# 044–29765, FUJIFILM Wako Pure Chemical and Cat# 11320033, Thermo Fisher Scientific) supplemented with N2 (Cat# 141–08941, FUJIFILM Wako Pure Chemical), B-27 Supplement Minus Vitamin A (Cat# 12587001, Thermo Fisher Scientific), ascorbic acid (50 μg/mL, Cat# ST-72132, STEMCELL Technologies), 1× GlutaMAX (Cat# 35050-061, Thermo Fisher Scientific), 1% monothioglycerol (Cat# 195–15791, FUJIFILM Wako Pure Chemical), 0.05% bovine serum albumin (Cat# 820024, Sigma-Aldrich), and 1× penicillin/streptomycin). During days 0–3 of differentiation, cells were cultured with SFD medium supplemented with 10 μM Y-27632 and 100 ng/mL recombinant Activin A (Cat# 338-AC-01M, R&D Systems) and 2% FBS. During days 3–5 of differentiation, cells were cultured in SFD medium supplemented with 1.5 μM Dorsomorphin dihydrochloride (Cat# 047–33763, FUJIFILM Wako Pure Chemical) and 10 μM SB431542 (Cat# 037–24293, FUJIFILM Wako Pure Chemical) for 24 h, and then SFD medium supplemented with 10 μM SB431542 and 1 μM IWP2 (Cat# 04–0034, Stemolecule) for another 24 h. During days 5–12 of differentiation, cells were cultured with SFD medium supplemented with 3 μM CHIR99021 (Cat# 034–23103, FUJIFILM Wako Pure Chemical), 10 ng/mL human FGF10 (Cat# AF-100-26, PeproTech), 10 ng/mL human FGF7 (Cat# AF-100-19, PeproTech), 10 ng/mL human BMP4 (Cat# 120-05ET, PeproTech), 20 ng/mL human EGF (Cat# AF-100-15, PeproTech), and all-trans retinoic acid (Cat# R2625 ATRA, Sigma-Aldrich). On day 12 of differentiation, cells were dissociated and embedded in Matrigel Growth Factor Reduced Basement Membrane to generate organoids. During days 12–20 of differentiation, cells were cultured in SFD medium containing 3 μM CHIR99021, 10 ng/mL human FGF10, 10 ng/mL human FGF7, 10 ng/mL human BMP4, and 50 nM ATRA. On day 20 of differentiation, organoids were recovered from the Matrigel, and the resulting organoid suspension (small free-floating clumps) was seeded onto Matrigel-coated cell culture plates. During days 20–30 of differentiation, cells were cultured in SFD medium containing 50 nM dexamethasone (Cat# S1322, Selleck Chemicals), 0.1 mM 8-bromo-cAMP (Cat# 1140/50, Tocris Bioscience), and 0.1 mM IBMX (3-isobutyl-1-methylxanthine) (Cat# 095–03413, FUJIFILM Wako Pure Chemical).

METHOD DETAILS

SARS-CoV-2 isolation

SARS-CoV-2 was isolated from the patient swabs on days 0, 17, 56, and 119. SARS-CoV-2 was isolated and replicated in TMPRSS2/Vero cells (Cat# JCRB1818, JCRB Cell Bank)[27] and stored at −80°C. TMPRSS2/Vero cells were cultured with Eagle's Minimum Essential Media (EMEM, Cat# 051–07615, FUJIFILM Wako Pure Chemical) supplemented with 5% fetal bovine serum (FBS) and 1% penicillin/streptomycin. All viral infection experiments were performed in a biosafety level 3 facility at Kyoto University under strict regulations.

SARS-CoV-2 genome analysis

Viral genome sequencing was performed as previously described.[32] Briefly, viral sequences were verified by viral RNA-sequencing analysis. Viral RNA was extracted using a QIAamp viral RNA mini kit (Cat# 52906, Qiagen). The sequencing library employed for total RNA sequencing was prepared using the NEBNext Ultra RNA Library Prep Kit for Illumina (Cat# E7530, New England Biolabs). Paired-end 76-bp sequencing was performed using a MiSeq system (Illumina) with MiSeq reagent kit v3 (Cat# MS-102-3001, Illumina). Sequencing reads were trimmed using fastp v0.21.0[28] and subsequently mapped to the viral genome sequences of a lineage B isolate (strain Wuhan-Hu-1; GenBank accession number: NC_045512.2)[27] using BWA-MEM v0.7.17.[29] Variant calling, filtering, and annotation were performed using SAMtools v1.9[30] and snpEff v5.0e.[31] SARS-CoV-2 genome sequences were obtained from nasopharyngeal swab specimens (D0: EPI_ISL_18890741, D17: EPI_ISL_18890742, D56: EPI_ISL_18890743, D119: EPI_ISL_18890744) and isolates (D0: EPI_ISL_18909991, D17: EPI_ISL_18910061, D56: EPI_ISL_18910100, D119: EPI_ISL_18910101).

SARS-CoV-2 titration

Viral titers were measured by a median tissue culture infectious dose (TCID50) assay. TMPRSS2/Vero cells[27] were cultured with EMEM and seeded into 96-well cell culture plates (Cat# 167008, Thermo Fisher Scientific). Samples were serially diluted 10-fold from 10^{-1} to 10^{-8} in cell culture medium, transferred onto TMPRSS2/Vero cells in triplicate, and incubated at 37°C for 96 h. Cytopathic effects were evaluated under a microscope. TCID50/mL was calculated using the Reed-Muench method.

Quantification of viral RNA copy number

Cell culture supernatants were mixed with an equal volume of 2× RNA lysis buffer (distilled water containing 0.4 U/μL SUPERase I RNase Inhibitor (Cat# AM2696, Thermo Fisher Scientific), 2% Triton X-100 (Cat# 35501-15, Nacalai Tesque), 50 mM KCl (Cat# 13091-75, Nacalai Tesque), 100 mM Tris-HCl (pH 7.4, Cat# 318–90225, NIPPON GENE), and 40% glycerol (Cat# 17017-93, Nacalai Tesque) and incubated at room temperature for 10 min. The mixture was diluted 10 times with distilled water. For quantification of SARS-CoV-2 RNA, a One Step TB Green PrimeScript PLUS RT-PCR Kit (Perfect Real Time) (Cat# RR096A, Takara Bio) was used on a QuantStudio 1 or QuantStudio 3 real-time PCR system (Thermo Fisher Scientific). Standard curves were prepared using SARS-CoV-2 RNA (10^5 copies/μL) purchased from Nihon Gene Research Laboratories. Primer sequences are shown in Table S1.

Antiviral drug/antibody assay using SARS-CoV-2 isolates and human iPS cell-derived lung organoids

Human iPS cell-derived lung organoids were infected with SARS-CoV-2 isolated obtained from the persistent COVID-19 patient. Cells were washed with EMEM and cultured in EMEM supplemented with 5% FBS, 1% penicillin/streptomycin, and serially diluted remdesivir (Cat# A17170, Clinisciences) or sotrovimab (Cat# HY-P99340, MedChemExpress). At 48 h after infection, cell culture supernatants were collected, and viral RNA was quantified using qPCR (see "quantification of viral RNA copy number" section above). The assay of each compound was performed in triplicate, and the 50% effective concentration (EC50) was calculated using Prism 9 software v9.1.1 (GraphPad Software).

RT-qPCR

Total RNA was isolated from respiratory organoids using ISOGENE (Cat# 319–90211, NIPPON GENE). cDNA was synthesized using 500 ng of total RNA with a Superscript VILO cDNA Synthesis Kit (Cat# 11754250, Thermo Fisher Scientific). Real-time RT-PCR was performed with SYBR Green PCR Master Mix (Cat# 4385614, Thermo Fisher Scientific) using a StepOnePlus real-time PCR system, QuantStudio 1, or QuantStudio 3 real-time PCR system (Thermo Fisher Scientific). The relative quantification of target mRNA expression was performed using the $2^{-\Delta\Delta CT}$ method. Values were normalized to the housekeeping gene *glyceraldehyde 3-phosphate dehydrogenase* (*GAPDH*). PCR primer sequences are shown in Table S2.

Measurement of the concentration of IgG antibody against SARS-CoV-2 S-RBD

To measure the concentration of IgG antibody against SARS-CoV-2 S-RBD, the serum collected from the persistent COVID-19 patient was analyzed using Anti-SARS-CoV-2 S-RBD protein Human IgG ELISA Kit (Cat# KE30003, Proteintech). ELISA was performed according to the manufacturer's instructions.

Measurement of cytokines in serum

To measure the concentration of cytokines, the serum collected from the persistent COVID-19 patient was analyzed using the Human Anti-Virus Response Panel (Cat# 740349, BioLegend) and Human CD8/NK Panel (Cat #740267, BioLegend). Flow cytometry was performed according to the manufacturer's instructions using MACSQuant Analyzer 10 Flow Cytometer (Milteniyi Biotec).

QUANTIFICATION AND STATISTICAL ANALYSIS

Statistical significance was evaluated using one-way analysis of variance (ANOVA) followed by Dunnett post hoc tests using GraphPad Prism 9. Data are representative of three independent experiments. Details are described in the figure legends.